

Magnetic Dynamics of La_2CuO_4 and $\text{La}_{2-x}\text{Ba}_x\text{CuO}_4$

G. Aeppli,^(1,2) S. M. Hayden,⁽³⁾ H. A. Mook,⁽⁴⁾ Z. Fisk,⁽⁵⁾ S.-W. Cheong,⁽⁵⁾ D. Rytz,⁽⁶⁾ J. P. Remeika,^{(1),(a)} G. P. Espinosa,⁽¹⁾ and A. S. Cooper⁽¹⁾

⁽¹⁾*AT&T Bell Laboratories, Murray Hill, New Jersey 07974*

⁽²⁾*Risø National Laboratory, Roskilde, DK-4000, Denmark*

⁽³⁾*Institut Laue-Langevin, 38042 Grenoble, France*

⁽⁴⁾*Oak Ridge National Laboratory, Oak Ridge, Tennessee 37831*

⁽⁵⁾*Los Alamos National Laboratory, Los Alamos, New Mexico 87545*

⁽⁶⁾*Hughes Research Laboratory, Malibu, California 90265*

(Received 27 February 1989)

High-energy inelastic neutron scattering is used to resolve spin waves in La_2CuO_4 . The corresponding long-wavelength velocity is $0.85 \pm 0.03 \text{ eV \AA}$, well above previous bounds set by thermal neutron scattering. Within experimental error, conventional spin-wave theory gives an excellent description of the magnetic dynamics for momentum and energy transfers below 0.15 \AA^{-1} and 0.1 eV , respectively. Doping with Ba changes the magnetic dynamics; the data indicate a combination of spin-wave softening and damping effects.

PACS numbers: 75.30.Ds, 71.30.+h, 74.70.Vy, 75.50.Ee

Because of high-temperature superconductivity in related oxides, the magnetism of $\text{La}_{2-x}(\text{Ba},\text{Sr})_x\text{CuO}_4$ has drawn considerable attention. In addition to many bulk measurements,¹ several microscopic techniques, notably light scattering,² muon spin relaxation,³ and thermal neutron scattering,^{4,5} have been used to probe the magnetic correlations in these materials. Unfortunately, however, due to restrictions in range (for both momentum and energy transfer) and resolution, magnetic excitations near the antiferromagnetic zone center have not been characterized quantitatively. In the present paper, we describe an epithermal neutron scattering experiment where the momentum resolution and incident beam energies are sufficient both to yield a value (not merely a lower bound) for the long-wavelength spin-wave velocity c and to permit comparison with conventional spin-wave theory for energy transfers up to $\hbar\omega = 0.1 \text{ eV}$. We also show that for $\hbar\omega \geq 0.03 \text{ eV}$, the magnetic fluctuations change little, if at all, on cooling through the Néel temperature from 290 to 5 K. Thus, for $\hbar\omega > kT$, paramagnetic La_2CuO_4 is not qualitatively different from an ordered antiferromagnet. Doping with Ba seems to result in softening of the spin waves, much as occurs on increasing δ in $\text{La}_2\text{NiO}_{4+\delta}$.⁶ Also interesting are indications of substantial spin-wave damping in Ba-doped La_2CuO_4 , an effect which has not (yet) been observed for $\text{La}_2\text{NiO}_{4+\delta}$.

Preliminary measurements were performed on crystals grown from a PbO flux. These are consistent with the more extensive measurements reported here and carried out for crystals obtained from melts containing excess CuO. The $\text{La}_{2-x}\text{Ba}_x\text{CuO}_{4-\delta}$ crystals were grown by top-seeding a solution of 0.85 CuO and $0.15 \text{ La}_{1.8}\text{Ba}_{0.2}\text{CuO}_4$. The morphology of the samples varied, with the La_2CuO_4 crystals being plates, with dimensions of order $15 \times 15 \times 1.5 \text{ mm}^3$, containing both orthorhombic

twins; the $\text{La}_{2-x}\text{Ba}_x\text{CuO}_{4-\delta}$ crystals had dimensions $\sim 8 \times 9 \times 3 \text{ mm}^3$. Inductively coupled plasma spectroscopy showed that the Ba content of the doped crystals was $x = 0.05 \pm 0.003$, while scanning microprobe analysis (beam diameter $\cong 1 \text{ }\mu\text{m}$) indicated that the Ba is uniformly distributed; neutron activation analysis gave $\delta \lesssim 0.1$. We mounted seven La_2CuO_4 crystals (total sample volume $\cong 2 \text{ cm}^3$) together so that their in-plane axes coincided to within better than 1° . Three crystals were used to yield a smaller sample of $\text{La}_{1.95}\text{Ba}_{0.05}\text{CuO}_4$.

Following previous practice,^{4,5} we label points in reciprocal space such that the basal planes are parallel to the $(h0l)$ zone, which in the inelastic experiments was also parallel to the horizontal scattering plane. The room-temperature lattice parameters (determined by x-ray diffraction) were $a = 5.375(2)$ and $5.357(3) \text{ \AA}$, $b = 13.156(4)$ and $13.165(5) \text{ \AA}$, and $c = 5.409(2)$ and $5.399(3) \text{ \AA}$ for the $x=0$ and 0.05 samples, respectively. For the pure sample, measurements of the elastic Bragg scattering showed a Néel temperature of $265 \pm 5 \text{ K}$, and saturation of the magnetic order for $T \lesssim 200 \text{ K}$. For $\text{La}_{1.95}\text{Ba}_{0.05}\text{CuO}_4$, magnetic Bragg scattering sets in at 150 K , reaches its maximum at 30 K [near the minimum ($0.1 \text{ }\Omega\text{cm}$) in the resistivity], below which it is reduced in the manner familiar from studies of reentrant spin glasses.⁷

We performed our inelastic experiments using the triple-axis spectrometer IN1 at the hot neutron source of the Institut Laue-Langevin (ILL). The hot source is a block of graphite, heated by γ radiation from the reactor, which thermalizes the neutrons so that their energy distribution is a Maxwellian with a maximum at 0.5 eV rather than the usual ("thermal") 0.05 eV . For all of our measurements, we used a vertically bent Cu(200) monochromator. The final energies were fixed at 0.08 and 0.15 eV , with vertically bent pyrolytic graphite (002)

and Cu(200) crystals used as analyzers, respectively. The filters to eliminate higher-order contamination were a 0.4-mm-thick sheet of Er in front of the sample (for $E_f=0.08$ eV), and 0.5 mm of Hf before and 0.4 mm of Er after the sample for $E_f=0.15$ eV.

Triple-axis neutron scattering data are typically collected to yield scans as a function of momentum (q) or energy ($\hbar\omega$) transfer for fixed $\hbar\omega$ or q , respectively. Considerations of resolution and background determine which type of scan is most appropriate. For steep dispersion curves, as illustrated in the inset of Fig. 1, it is best to vary q for fixed $\hbar\omega$, i.e., to perform scans in $\hbar\omega$ - q space following the dashed rather than dotted line. For the antiferromagnetic (AFM) spin-wave branches shown near the (AFM) zone center ($q=0$), there will be two maxima in constant- $\hbar\omega$ (for large $\hbar\omega$) spectra, due to spin waves propagating in opposite directions. For lower $\hbar\omega$, the two maxima coalesce because the resolution volume can simultaneously enclose all scattering from magnons with energy $\hbar\omega$. The inability of thermal (low $\hbar\omega$) neutron scattering to provide anything other than a lower bound on the spin-wave velocity c is due to this effect.

Figure 1 shows a transverse scan through $Q_0=(2,0,1)$ for $\hbar\omega=0.1$ eV. As expected, there are two maxima, lo-

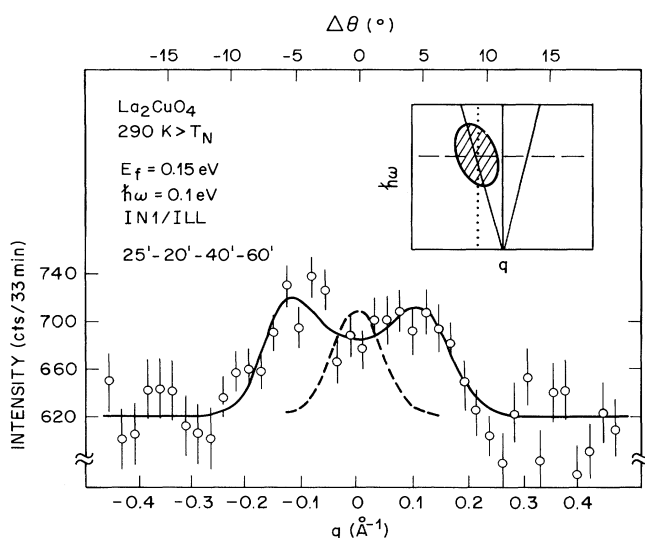


FIG. 1. Constant-energy scan collected in transverse direction for momentum transfers near $Q_0=(2,0,1)$; q and $\Delta\theta$ represent deviations from Q_0 in scattering vector and sample angle, respectively. Dashed line corresponds to resolution-corrected cross section calculated for spin waves with infinite velocity, while solid line represents best fit by spin-wave theory described in text. Inset indicates schematically how antiferromagnetic spin-wave dispersion surface is crossed in $\hbar\omega$ - q plane via constant- q (dotted line) and constant- $\hbar\omega$ (dashed line) scans; the hatched area represents the resolution ellipse of the instrument.

cated at $q \approx \pm 0.1 \text{ \AA}^{-1}$. The dashed line represents the (calculated) response of the instrument for the case of infinite spin-wave velocity, while the solid line corresponds to the best fit obtainable assuming spin waves with zero damping and a finite velocity ($\hbar c = 0.78 \pm 0.04 \text{ eV \AA}$). In the long-wavelength limit, the cross section for conventional antiferromagnetic spin waves is⁸

$$\frac{\partial^2 \sigma}{\partial \Omega \partial \omega} = \frac{k_f}{k_i} A_q \{ [n(cq) + 1] \delta(\omega - cq) + n(cq) \delta(\omega + cq) \}, \quad (1)$$

where k_i and k_f are the wave vectors of the ingoing and outgoing neutrons, respectively, $n(\omega)$ is the Bose-Einstein occupation factor $[\exp(\beta\hbar\omega) - 1]^{-1}$, and $A_q \sim 1/q$ is the square of the transition matrix element connecting the Néel state to one spin wave with wave vector q . Figure 2 shows the fitted amplitudes and spin-wave eigenvectors ($\omega/c = q$) as a function of the energies $\hbar\omega$ fixed in scans like that of Fig. 1. The solid and dashed lines represent the predictions of conventional spin-wave theory [Eq. (1)] for $T=5 \text{ K}$ ($\ll T_N=265 \text{ K}$) and 290 K ($> T_N$), respectively: q rises linearly with $\hbar\omega$ over the

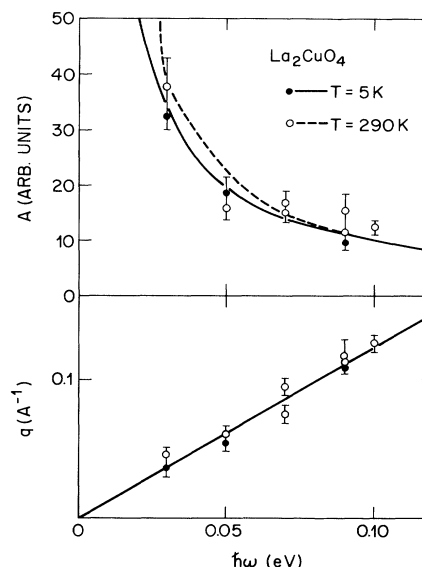


FIG. 2. Fitted spin-wave amplitudes (upper frame) and wave vectors (lower frame) obtained for a variety of constant- $\hbar\omega$ scans at 5 and 290 K. Dashed and solid curves are derived from conventional spin-wave theory. Data for $\hbar\omega=0.03$ eV were taken near $Q_0=(1,0,0)$; all other data were collected near $Q_0=(2,0,1)$. To place data on the same scale, amplitudes were corrected using the Freeman-Watson Cu^{2+} form factor, which is consistent with existing static form-factor data for La_2CuO_4 (Ref. 4). Differing analyzer efficiencies were also taken into account using the scale factor measured for spin-wave scattering at $\hbar\omega=70$ meV with the two different analyzer-final-energy combinations described in text.

entire range probed, while the overall amplitude $A \sim [n(\omega) + 1](1/q)$. It is clear that the data are in very good agreement with conventional theory. In particular, there is no need to introduce novel fluctuation (e.g., "quantum spin fluid"⁵) or lifetime effects to understand the magnetic dynamics for wavelengths longer than 10 Å and energies below 0.1 eV. The results are quite insensitive to temperature, which implies that at the wave vectors and energies probed, the system always behaves as an ordered magnet. This should not be surprising even for $T = 290$ K, given that the lowest $\hbar\omega$ (30 meV) is still somewhat larger than kT and that the two-dimensional correlation lengths ξ reported for La_2CuO_4 with $T \gtrsim T_N$ are very long.⁵ Of course, for $\hbar\omega < kT$ and $q \lesssim \xi^{-1}$, order-parameter relaxation rather than spin-wave propagation is expected to dominate, as for any classical antiferromagnet with $T > T_N$.⁹

At 5 K, the spin-wave velocity obtained from our data is $\hbar c = 0.85 \pm 0.03$ eV Å, well above the highest lower bound (0.6 eV Å) based on thermal neutron scattering measurements.⁵ To interpret this result, we consider the Heisenberg Hamiltonian,

$$H = \sum_{\langle i,j \rangle} J S_i \cdot S_j, \quad (2)$$

where the sum is over nearest-neighbor pairs $\langle i,j \rangle$ of spins S_i, S_j and J is the antiferromagnetic exchange coupling. According to standard theory, the spin-wave velocity $c = SJZa/\sqrt{2}$, where Z is the number of nearest neighbors of a given spin. In the case of La_2CuO_4 , $S = \frac{1}{2}$, the lattice parameter $a = 3.79$ Å, and $Z = 4$, and so our measured value of c corresponds to $J = 0.16$ eV. The exchange constant derived from two-magnon Raman scattering² is 0.14 eV, which is somewhat smaller. This discrepancy is not significant, especially in view of the uncertainty in the amount by which the peak in the two-magnon spectrum is shifted from $2SJZ$. Furthermore, recent theoretical work¹⁰ suggests that for the square lattice $S = \frac{1}{2}$, c is renormalized upwards by 18% with respect to the conventional value of $Ja\sqrt{2}$.

We now shift our attention to the lightly doped sample, $\text{La}_{1.95}\text{Ba}_{0.05}\text{CuO}_4$. Figure 3 shows scans taken for $\hbar\omega = 30$ and 50 meV and, for comparison, an $\hbar\omega = 30$ meV scan taken at the same temperature for our pure La_2CuO_4 sample. In addition, the lowermost scan in frame (a) is obtained in the two-axis manner (i.e., no energy analysis of the neutrons scattered by the sample) where an integral is performed over outgoing neutron energies with the in-plane component of the momentum transfer fixed. The resulting intensities are roughly proportional to an integral of the magnetic structure factor

$$\frac{\partial^2 \sigma}{\partial \Omega \partial \omega} = \frac{k_f}{k_i} A_1 [1 - \exp(-\beta \hbar \omega)]^{-1} \frac{\omega \Gamma}{\pi} \left[\frac{1}{(\omega - qc)^2 + \Gamma^2} + \frac{1}{(\omega + cq)^2 + \Gamma^2} \right]. \quad (3)$$

Note that if the spin-wave decay rate $\Gamma \rightarrow 0$, Eq. (3) reduces to Eq. (1) with $A_q = \omega A_1$. On the other hand, for $c \rightarrow 0$,

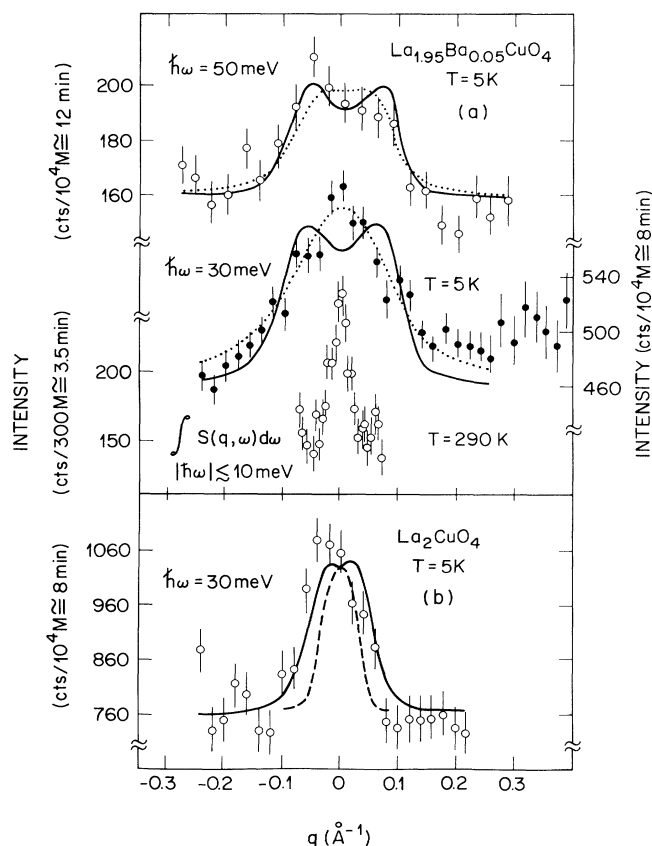


FIG. 3. (a) Constant $\hbar\omega = 30$ - and 50-meV scans for $\text{La}_{1.95}\text{Ba}_{0.05}\text{CuO}_4$ compared to double-axis scan (measuring fluctuations with $\hbar\omega \lesssim 10$ meV) for the same compound, and (b) constant $\hbar\omega = 30$ meV scan for La_2CuO_4 . Dashed line in (b) corresponds to spin waves with infinite velocity, and dotted and solid lines are derived from fits described in text.

$S(q, \omega)$ for $|\hbar\omega| \lesssim 10^{-2}$ eV; note that these measurements, like those reported elsewhere^{5,6} for $\text{La}_{2-x}\text{Sr}_x\text{CuO}_4$ and $\text{La}_2\text{NiO}_{4+\delta}$, were performed using thermal neutrons (the incident energy was 14.7 meV). The corresponding magnetic correlation length, found from the width of our two-axis scan, is $\xi \approx 50$ Å.

Returning to the inelastic measurements, the most important conclusion to draw from Fig. 3 is that the spectra are broader than for the undoped case, implying either increased damping of the spin waves and/or a reduction in their velocities. Furthermore, the broadening is apparent at wave vectors large compared to ξ^{-1} . In other words, doping affects the dynamics even for $q \gtrsim 5\xi^{-1}$. To decide whether damping or softening dominates, we have analyzed the data using the following cross section:

the right-hand side of Eq. (3) becomes (for $T=0$ and $\omega > 0$) $(k_f/k_i)A_1\Gamma\omega/(\Gamma^2+\omega^2)$, a form familiar from studies of Kondo, mixed-valence, and heavy-fermion systems. The solid lines in Fig. 3 correspond to the best fits to the data of Eq. (3), with $\hbar\Gamma$ fixed at 5 meV, a value indistinguishable from zero in these measurements. This procedure yields a good description of the data for $\hbar\omega=50$ meV; the resulting spin-wave velocity is $\hbar c=0.63\pm0.05$ eV Å, significantly below the value, 0.85 ± 0.03 eV Å, found for pure La_2CuO_4 . Reductions of c with increasing metallicity have been inferred from neutron scattering experiments on $\text{La}_2\text{Ni-O}_{4+\delta}$ (Ref. 6) and bulk susceptibility¹¹ and muon spin relaxation data³ for $\text{La}_{2-x}\text{Sr}_x\text{CuO}_4$.

For $\hbar\omega=30$ meV, the $\text{La}_{1.95}\text{Ba}_{0.05}\text{CuO}_4$ data can also be fitted assuming sharp spin waves (solid line in Fig. 3), but the results are not as satisfactory as for $\hbar\omega=50$ meV. The second fitting procedure, whose outcomes are represented by the dotted lines in Fig. 3, involves fixing c at the value for the pure compound and varying $\hbar\Gamma$. This provides a considerably better description of the 30-meV data, but, if distinguishable at all, a slightly worse account of the behavior at 50 meV. For 30 meV, the optimal $\hbar\Gamma=22\pm4$ meV, which means that the spin waves here are essentially overdamped.

Clearly, more experiments are required to determine quantitatively the relative importance of softening and damping effects, and to decide whether it is the appearance of (weakly localized) carriers or simple disorder, as might be found in insulating random magnets,⁷ which accounts for our observations on $\text{La}_{1.95}\text{Ba}_{0.05}\text{CuO}_4$. In this regard, we note that the energies of the fluctuations probed in the present inelastic experiment correspond to temperatures more than an order of magnitude larger than that at which (~ 30 K) the resistance minimum for the compound occurs. Furthermore, while yielding substantial spin-wave softening, doping has not yet been found to produce visible damping in La_2NiO_4 .⁶

In summary, we have performed the first neutron scattering measurements on $\text{La}_{2-x}\text{Ba}_x\text{CuO}_4$ at energy transfers comparable to the pair-breaking energies found for typical high- T_c superconductors and sufficiently large to allow the determination of the spin-wave velocity c . For La_2CuO_4 , we find that $\hbar c=0.85\pm0.03$ eV Å. Furthermore, in agreement with recent calculations,^{9,12} conventional spin-wave theory gives an excellent description of all of our data for $kT\lesssim\hbar\omega\leq 0.1$ eV. Unusual quantum effects are present neither above nor below T_N , although refined measurements with considerably better resolution and statistics should eventually reveal corrections¹³ to ordinary spin-wave theory. Results for $\text{La}_{1.95}\text{Ba}_{0.05}\text{CuO}_4$ show that doping affects the magnetic

dynamics at wavelengths short compared to the static (measured for energy transfers below 10 meV) magnetic correlation length. Analysis of the limited data set current available indicates that a combination of spin-wave softening and damping is responsible for the differences in the dynamics of the pure and doped compounds. We anticipate that further work¹⁴ on Hubbard models with small deviations from half filling will help to decide whether the decay of spin waves into electron-hole pairs leads to the effects found for $\text{La}_{1.95}\text{Ba}_{0.05}\text{CuO}_4$.

It is a pleasure to thank B. Dörner for advice and assistance on IN1, J. Budai and E. Sönder for lattice parameter and resistivity measurements on $\text{La}_{1.95}\text{Ba}_{0.05}\text{CuO}_4$, C. Chaillout and M. Marezio for the lattice parameter determination for La_2CuO_4 , and C. Broholm for technical help at the beginning of this project. We are also grateful to D. Huse, D. C. Johnston, G. Reiter, and C. M. Varma for helpful discussions, and P. Fleury for a critical reading of the manuscript. The U.S. Department of Energy funded work at Oak Ridge (Contract No. DE-AC05-84OR21400 with Martin Marietta Energy Systems) and Los Alamos National Laboratories.

^(a)Deceased.

¹L. F. Schneemeyer *et al.*, Phys. Rev. B **35**, 8421 (1987); Y. Yamaguchi *et al.*, Jpn. J. Appl. Phys. Pt. 2 **26**, L477 (1987); R. L. Greene *et al.*, Solid State Commun. **63**, 379 (1987).

²K. Lyons *et al.*, Phys. Rev. B **37**, 2353 (1988).

³D. Harshman *et al.*, Phys. Rev. B **38**, 852 (1988); J. Budnick *et al.*, Europhys. Lett. **5**, 651 (1988); Y. Uemura *et al.*, Phys. Rev. Lett. **59**, 1045 (1987).

⁴D. Vaknin *et al.*, Phys. Rev. Lett. **58**, 2802 (1987); T. Freltoft *et al.*, Phys. Rev. B **37**, 137 (1988).

⁵R. J. Birgeneau *et al.*, Phys. Rev. B **38**, 6614 (1988).

⁶G. Aeppli and D. Buttrey, Phys. Rev. Lett. **61**, 203 (1988); T. Freltoft *et al.* (unpublished).

⁷See, e.g., the review by S. M. Shapiro *et al.*, Physica (Amsterdam) **137B**, 96 (1987).

⁸A discussion of neutron scattering from antiferromagnets is given by S. W. Lovesey, *Theory of Neutron Scattering from Condensed Matter* (Clarendon, Oxford, 1984).

⁹S. Tyc, B. I. Halperin, and S. Chakravarty, Harvard University report, 1988 (to be published).

¹⁰R. Singh, AT&T Bell Laboratories report, 1989 (to be published).

¹¹D. C. Johnston, Ames Laboratory report, 1988 (to be published).

¹²A. Auerbach and D. Arovas, Phys. Rev. Lett. **61**, 617 (1988).

¹³G. Reiter (private communication).

¹⁴Recent attempts to deal with this problem include those by S. Schmitt-Rink, C. M. Varma, and A. E. Ruckenstein, Phys. Rev. Lett. **60**, 2793 (1988), and by B. I. Shraiman and E. D. Siggia, Phys. Rev. Lett. **61**, 467 (1988).